



**HAL**  
open science

# Nonadiabatic Coupling in Trajectory Surface Hopping: Accurate Time Derivative Couplings by the Curvature-Driven Approximation

Xiaorui Zhao, Isabella Merritt, Ruiqing Lei, Yinan Shu, Denis Jacquemin,  
Linyao Zhang, Xuefei Xu, Morgane Vacher, Donald Truhlar

► **To cite this version:**

Xiaorui Zhao, Isabella Merritt, Ruiqing Lei, Yinan Shu, Denis Jacquemin, et al.. Nonadiabatic Coupling in Trajectory Surface Hopping: Accurate Time Derivative Couplings by the Curvature-Driven Approximation. *Journal of Chemical Theory and Computation*, 2023, 19 (19), pp.6577-6588. 10.1021/acs.jctc.3c00813 . hal-04753545

**HAL Id: hal-04753545**

**<https://hal.science/hal-04753545v1>**

Submitted on 25 Oct 2024

**HAL** is a multi-disciplinary open access archive for the deposit and dissemination of scientific research documents, whether they are published or not. The documents may come from teaching and research institutions in France or abroad, or from public or private research centers.

L'archive ouverte pluridisciplinaire **HAL**, est destinée au dépôt et à la diffusion de documents scientifiques de niveau recherche, publiés ou non, émanant des établissements d'enseignement et de recherche français ou étrangers, des laboratoires publics ou privés.

# Nonadiabatic Coupling in Trajectory Surface Hopping: Accurate Time Derivative Couplings by the Curvature-Driven Approximation

Xiaorui Zhao,<sup>1,2,⊥</sup> Isabella C. D. Merritt,<sup>3,⊥</sup> Ruiqing Lei,<sup>1</sup> Yinan Shu,<sup>4</sup> Denis Jacquemin,<sup>3,5</sup> Linyao Zhang,<sup>6,\*</sup> Xuefei Xu,<sup>1,7,\*</sup> Morgane Vacher,<sup>3,\*</sup> and Donald G. Truhlar<sup>4,\*</sup>

<sup>1</sup> Center for Combustion Energy, Tsinghua University, Beijing 100084, P. R. China

<sup>2</sup> School of Aerospace Engineering, Tsinghua University, Beijing 100084, P. R. China

<sup>3</sup> Nantes Université, CNRS, CEISAM UMR 6230, F-44000 Nantes, France

<sup>4</sup> Department of Chemistry, Chemical Theory Center, and Supercomputing Institute, University of Minnesota, Minneapolis, MN 55455-0431, USA

<sup>5</sup> Institut Universitaire de France (IUF), 75005 Paris, France

<sup>6</sup> School of Energy Science and Engineering, Harbin Institute of Technology, Harbin 150001, P. R. China

<sup>7</sup> Department of Energy and Power Engineering, and Key Laboratory for Thermal Science and Power Engineering of Ministry of Education, Tsinghua University, Beijing 100084, P. R. China

⊥ X. Z. and I. C. D. M. contributed equally.

\*Corresponding authors: [truhlar@umn.edu](mailto:truhlar@umn.edu), [morgane.vacher@univ-nantes.fr](mailto:morgane.vacher@univ-nantes.fr), [xuxuefei@tsinghua.edu.cn](mailto:xuxuefei@tsinghua.edu.cn), [zhanglinyao1209@gmail.com](mailto:zhanglinyao1209@gmail.com)

**Abstract.** Trajectory surface hopping (TSH) is a widely used mixed quantum-classical dynamics method, which is used to simulate molecular dynamics with multiple electronic states. In TSH, the time-derivative coupling (TDC) is employed to propagate the electronic coefficients and in that way to determine when the electronic state on which the nuclear trajectory is propagated switches. In this work, we discuss nonadiabatic TSH dynamics algorithms employing curvature-driven approximation and overlap-based time derivative couplings, and we report test calculations on six photochemical reactions where we compare the results to one another and to calculations employing analytic nonadiabatic coupling vectors. We correct previous published results, thanks to a bug found in the software. We also provide additional more detailed studies of the time derivative couplings. Our results show good agreement between curvature-driven algorithms and overlap-based algorithms.

## 1. Introduction

In a recently published work<sup>1</sup>, some of the current authors reported a benchmark study on the accuracy of various approximations to the time-derivative coupling (TDC) that governs electronic-wave-function-propagation algorithm in nonadiabatic dynamics calculations carried out by trajectory surface hopping<sup>2,3,4,5</sup> (TSH). One of the conclusions was that the curvature-driven approximation to the TDC<sup>6,7,8</sup> that was implemented in SHARC-MN v1.2 deviates from most of the other algorithms. Unfortunately, this was due to a bug in SHARC-MN v1.2. In this work, we show the high accuracy of the curvature-driven approximation, correcting the original conclusion. We also present additional discussion of various approximations to the TDC.

The deviation reported in ref. 1 was caused by a bug in SHARC-MN v1.2 in evaluating the curvature-driven time-derivative coupling ( $\kappa$ TDC) by second-order finite differences of energies, which we will call the energy formula. An alternative formula, called the gradient formula, involves the dot product of the velocity and first-order finite differences of gradients. The previous works using curvature-driven approximations and the gradient formula with SHARC-MN were not affected by the bug. (To be perfectly clear: None of the published work of the Minnesota group is affected by the bug.) Although the approach for evaluating the  $\kappa$ TDC to be preferred is the gradient formula, we do show here that the energy formula is accurate as well. Both formulas are coded correctly in SHARC-MN v2.0<sup>9</sup> and SHARC 3.0,<sup>10</sup> either may be used in future work.

In addition to correcting the results of the earlier benchmark that were affected by the bug, the present paper reports more extensive studies on electronic propagation algorithms. Specifically, we will show the accuracy of  $\kappa$ TDC when compared to the analytic TDC evaluated from nonadiabatic coupling vectors (NACs).

## 2. Theoretical Background

The most efficient methods for simulating electronically nonadiabatic processes are semiclassical methods, in which the electronic structure is modeled quantum mechanically, and nuclear motion follows a semiclassical trajectory.<sup>11,12,13,14,15,16,17,18,19,20</sup> We consider calculations in the adiabatic representation, where the coupling of electronic states is due to the nonadiabatic coupling vector (NAC). We focus first on the coherent propagation of

electronic coefficients, but decoherence<sup>21</sup> will be added below. The key step in coherently propagating the electronic coefficients in a trajectory surface hopping calculation is to evaluate the TDC. There are three kinds of algorithms for this: (i) NAC-based algorithms that compute the TDC as a scalar product between the NAC and the velocity vector;<sup>4,22</sup> (ii) overlap-based algorithms approximate TDC by exact or approximate overlaps of electronic adiabatic wave functions at successive time steps<sup>23,24</sup> (in the following discussion, we will call simply label such integrals as the overlap integral); (iii) curvature-driven algorithms approximate the TDC in terms of derivatives the adiabatic potential energy surfaces.<sup>6,7,8</sup> (Algorithms that use nonadiabatic models – the original Landau–Zener model of Preston and Tully<sup>2</sup> or the Zhu–Nakamura model<sup>25</sup> – rather than propagating the electronic wave function are outside the scope of this discussion.)

NAC-based algorithms require computing NACs from electronic structure programs<sup>26,27</sup> or from fitted diabatic potential energy matrices;<sup>28</sup> overlap-based algorithms require computing adiabatic-wave-function overlap integrals,<sup>29</sup> thereby avoiding NAC calculations; and curvature-driven algorithms avoid both NACs and overlaps. Not only are curvature-driven algorithms more efficient, but also, they can be interfaced with electronic structure methods for which NACs are not available (e.g., multi-state pair density functional theory.<sup>30,31</sup>) or with machine-learned potentials for which the adiabatic wave functions are not available.<sup>32,33</sup>

We emphasize the distinction between the propagation algorithm and the way to approximate the TDC. For dynamics methods that do not use NACs, we use “t” and “κ” as prefixes to denote which kind of approximation is used. For example, tTSH denotes a TSH dynamics method that uses an overlap-based algorithm, and κTSH denotes a TSH method that uses a curvature-driven algorithm, whereas tCSDM and κCSDM denote using these kinds of algorithms in the coherent switching with decay of mixing<sup>34</sup> (CSDM) dynamics method.

Overlap-based algorithms are the most widely used due to their simplicity (they calculate only the one needed component of the NAC rather than all components followed by a scalar product to project out the component of interest) and due to their high accuracy for narrowly avoided crossings (or trivial crossings).<sup>35,36,37,38</sup> The overlap may be computed accurately<sup>29</sup> or by several approximation schemes. The conversion of an overlap integral to the TDC is called

---

an HST<sup>23</sup> scheme in ref. 1, and ref. 1 provides the accuracy of two ways to approximate the overlap integral. The first one named HST(CIV) utilizes coefficients of configuration state functions in a configuration interaction calculation (also called CI vectors).<sup>39</sup> The HST(CIV) scheme neglects the contribution to the overlap integrals from the changes in the difference in the molecular orbitals at successive steps. The alternative, called HST(BiO), approximates the overlap by using a biorthogonal transformation of orbitals<sup>40</sup> that is implemented in *OpenMolcas*<sup>41</sup> in Ref. 1. This is a better approximation because it includes the change in shape of the molecular orbitals, but it still neglects their translation due to the time step. As explained below, a related but more accurate approach than the HST scheme is to use the norm-preserving interpolation (NPI) scheme to evaluate the TDC.<sup>42</sup> In SHARC and SHARC-MN, the NPI scheme is combined with substep propagators; this combination constitutes the NPI algorithm.<sup>43</sup>

It has been proposed that the HST(CIV) scheme can be improved by diabaticizing the orbitals at the current time step to those at the previous time step<sup>44</sup> (available in *Molpro*,<sup>45</sup> basically a block diagonalization that is done by maximizing overlaps of orbitals for a reference geometry), but that is not employed here or in *OpenMolcas*.

Another way to use the overlap integrals is the local diabaticization method. In this approach, instead of using overlap integrals to calculate the TDC, one uses overlap integrals to construct a local diabatic representation, and one propagates electronic coefficients in the quasidiabatic basis.<sup>24</sup> This is called the local diabaticization (LD) scheme.<sup>1</sup> Technically, one is not approximating the TDC, but since the method is closely related to the overlap methods used to approximate the TDC, we include it in this category. This kind of local diabatic representation was introduced for time-dependent propagation in 2001,<sup>24</sup> but basically the same idea was introduced for time-independent propagation of wave functions much earlier.<sup>46</sup>

Next consider curvature-driven algorithms. There are two ways to approximate TDCs in curvature-driven algorithms,<sup>7</sup> one uses first-order finite differences on the scalar product of the gradient with the velocity vector (gradient formula),<sup>7</sup> and the other uses second-order finite differences of potential energies (energy formula).<sup>6,7,8</sup> The gradient formula appears to be numerically more stable, and it is the preferred method.<sup>6,47,48,49</sup> However, when employing TSH for internal conversion with propagation at any given time requiring the gradient of only

the active potential energy surface, the energy approach is more efficient because the gradient formula requires computing gradients of all electronic states. This advantage of the energy method is not present when one does  $\kappa$ CSDM<sup>7</sup> or when one calculates intersystem crossing.<sup>50,51</sup> (The reason why this advantage is not present for intersystem crossing calculations is that those calculations require all the gradients.<sup>51</sup>)

### 3. Sections

In the present work, we compare several schemes, included all three categories of algorithms, to investigate TSH nonadiabatic dynamics of six typical reaction systems. In section 4, we introduce the propagation of electronic coefficients and introduce various schemes and approximations for estimating the TDC. Section 5 provides some computational details. In section 6, we show two sets of simulation results; set 1 is used to test the accuracy of curvature-driven schemes, and set 2 is an investigation on how the curvature-driven approximation influences the nonadiabatic dynamics in detail. Section 7 has a summary of the conclusions.

### 4. Theory

This article is limited to internal conversion processes (processes that do not change the total electronic spin, which is assumed to be conserved), and in this section, we describe in detail the electronic propagators used in this work. Section 4.1 briefly recaps the electronic equation of motion. Section 4.2 summarizes the approximations to compute TDCs.

#### 4.1. Coherent Electronic Equation of Motion

The time-dependent wave function can be written as

$$\Psi = \sum_J c_J \phi_J \quad (1)$$

where  $\phi_J$  is a basis function, and  $c_J$  is an electronic state expansion coefficient. In the adiabatic representation the  $\phi_J$  are eigenfunctions of the electronic Hamiltonian, and the coherent electronic equation of motion in the electronically adiabatic representation is

$$[\dot{c}_I]_C = -\frac{i}{\hbar} \left( c_I V_I - i\hbar \sum_{J \neq I} c_J \sigma_{IJ} \right) \quad (2)$$

where an overdot denotes a time derivative,  $V_I$  is the adiabatic potential energy of state  $I$ ,  $[\dots]_C$  denotes the coherent time development, and  $\sigma_{IJ}$  is an element of the TDC matrix  $\sigma$  between

electronic states  $I$  and  $J$ ,

$$\sigma_{IJ} = \left\langle \phi_I \left| \frac{d}{dt} \right| \phi_J \right\rangle \quad (3)$$

The TDC can be written as

$$\sigma_{IJ} = \mathbf{d}_{IJ} \cdot \dot{\mathbf{R}} \quad (4)$$

where  $\dot{\mathbf{R}}$  is the nuclear velocity vector, and  $\mathbf{d}_{IJ}$  is the NAC between electronic states  $I$  and  $J$ ,

$$\mathbf{d}_{IJ} = \left\langle \phi_I \left| \frac{\partial}{\partial \mathbf{R}} \right| \phi_J \right\rangle \quad (5)$$

In labeling the various algorithms in the discussion below, we call direct use of eq (4) the analytic scheme for computing the TDC.

It is convenient to rewrite eq (2) in the more general matrix form

$$\dot{\mathbf{c}} = - \left( \frac{i}{\hbar} \mathbf{H}^{\text{elec}} + \boldsymbol{\sigma} \right) \mathbf{c} \quad (6)$$

where we dropped the subscript C to simplify the notation,  $\mathbf{H}^{\text{elec}}$  is the electronic Hamiltonian in a general basis (or, as we sometimes say, in a general representation), and  $\boldsymbol{\sigma}$  is the TDC matrix in that basis. When we use the adiabatic representation,  $\mathbf{H}^{\text{elec}}$  is diagonal, and the diagonal matrix elements are the adiabatic potential energies  $V_I$ . When we use a diabatic representation,  $\mathbf{H}^{\text{elec}}$  is a nondiagonal matrix called the diabatic potential energy matrix (DPEM). The diagonal and off-diagonal matrix elements of DPEM are called diabatic potentials and diabatic couplings respectively. A diabatic representation is one where we can safely approximate  $\boldsymbol{\sigma}$  as a zero matrix.<sup>52</sup> Therefore, in a diabatic representation, the population transfer between diabatic electronic states is driven by off-diagonal matrix elements of the DPEM.

Electronic structure programs provide electronic wave functions in the adiabatic representation, and to propagate the electronic state coefficients in the adiabatic representation, one needs to compute or approximate  $\boldsymbol{\sigma}$ . (The TDC can be neglected if one performs an adiabatic-to-diabatic transformation but the construction of global diabatic bases is laborious,<sup>52</sup> especially for large molecules, so this is not usually done.) Approximate methods for computing  $\boldsymbol{\sigma}$  are discussed in sections 4.2.1 to 4.2.3, and construction of locally diabatic states using the LD scheme is discussed in section 4.2.4.

## 4.2. Time Derivative Couplings

### 4.2.1. The Hammes-Schiffer–Tully Scheme

Hammes-Schiffer and Tully were the first to publish the relation shown in eq (4), and they proposed a scheme to compute the TDC using overlap integrals,<sup>23</sup>

$$S_{IJ}(t, t^+) = \left\langle \phi_I(t) \left| \phi_J(t^+) \right. \right\rangle \quad (7)$$

where

$$t^+ \equiv t + \Delta t \quad (8)$$

and where  $\phi_I(t)$  is the wave function of adiabatic electronic state  $I$  at time  $t$ ,  $\phi_J(t^+)$  is the wave function of adiabatic electronic state  $J$  at time  $t^+$ , and  $\Delta t$  is the time step to propagate the nuclear equation of motion (in some algorithms, the electronic equation of motion is also propagated with time step  $\Delta t$ ). The HST approximations are

$$\sigma_{IJ}^H \left( t + \frac{1}{2} \Delta t \right) = \frac{S_{IJ}(t, t^+) - S_{JI}(t, t^+)}{2\Delta t} \quad (9)$$

and

$$\sigma_{IJ}^H \left( t - \frac{1}{2} \Delta t \right) = \frac{S_{IJ}(t^-, t) - S_{JI}(t^-, t)}{2\Delta t} \quad (10)$$

where

$$t^- \equiv t - \Delta t \quad (11)$$

Therefore, one can approximate  $\sigma_{IJ}(\mathcal{T})$  for any point in the time interval  $t - \frac{1}{2} \Delta t \leq \mathcal{T} \leq t + \frac{1}{2} \Delta t$  by

$$\sigma_{IJ}^{\text{HST}}(\mathcal{T}) = \sigma_{IJ}^H \left( t - \frac{1}{2} \Delta t \right) + \frac{\mathcal{T} - \left( t - \frac{1}{2} \Delta t \right)}{\Delta t} \left( \sigma_{IJ}^H \left( t + \frac{1}{2} \Delta t \right) - \sigma_{IJ}^H \left( t - \frac{1}{2} \Delta t \right) \right) \quad (12)$$

Clearly, eq (12) linearly interpolates the TDC between two times, namely,  $t - \frac{1}{2} \Delta t$  and  $t + \frac{1}{2} \Delta t$ . One disadvantage of such a linear interpolation is that it might completely miss the peak of the TDC when a NAC is narrowly distributed. This would make the integration of electronic coefficients wrong. Such a problem is amplified for trivial crossing situations. This deficiency has stimulated methods like norm-preserving interpolation and local diabaticization algorithms, which will be discussed in later sections. When  $\mathcal{T} = t$ , this becomes

$$\sigma_{IJ}^{\text{HST}}(t) = \frac{S_{IJ}(t, t^+) - S_{JI}(t, t^+) + S_{IJ}(t^-, t) - S_{JI}(t^-, t)}{4\Delta t} \quad (13)$$

One can use approximated overlap integrals instead of true overlap integrals in HST



scheme. As reviewed in Section 2, computing overlap integrals using only configuration interaction coefficients generates the so-called HST(CIV) scheme, and using configuration interaction coefficients and biorthonormal orbitals generates the HST(BiO) scheme.

Because  $S_{IJ}(t, t^+)$  can be computed without computing NACs, the HST scheme, with either accurate or approximate overlap integrals, allows one to compute the TDC without computing NACs. In addition, the HST can alleviate the trivial crossing problem.<sup>42</sup> Therefore, HST scheme is widely used.<sup>35,36,53,54,55</sup>

#### 4.2.2. The Norm Preserving Interpolation Scheme

The accuracy of the HST scheme depends on the time step because of the linear interpolation. An improved version developed by Meek and Levine<sup>42</sup> and called norm-preserving interpolation (NPI), includes higher-order contributions. The HST scheme can be considered as a linear approximation to the NPI scheme. The NPI scheme approximates the evolution of the electronic wave function in the time interval  $t \leq \mathcal{T} \leq t^+$  by using a two-state rotation matrix at time  $\mathcal{T}$ :

$$\phi_I(\mathcal{T}) = \Theta(\mathcal{T})\phi_I(t) \quad (14)$$

where the elements of the rotation matrix  $\Theta(\mathcal{T})$  are

$$\Theta_{II}(\mathcal{T}) = \cos\left(\cos^{-1}\left(S_{IJ}(t, t^+)\right)\frac{\mathcal{T} - t}{\Delta t}\right) \quad (15)$$

$$\Theta_{IJ}(\mathcal{T}) = \sin\left(\sin^{-1}\left(S_{IJ}(t, t^+)\right)\frac{\mathcal{T} - t}{\Delta t}\right) \quad (16)$$

Therefore,

$$\sigma_{IJ}^{\text{NPI}}(\mathcal{T}) = \left\langle \phi_I(t) \left| \Theta^\dagger(\mathcal{T}) \frac{\partial}{\partial \mathcal{T}} \Theta(\mathcal{T}) \right| \phi_J(t) \right\rangle \quad (17)$$

The NPI scheme is a higher-order way to use overlap integrals without requiring NACs.

Although not implemented and never tested, one could imagine converting approaches like HST(CIV) and HST(BiO) to NPI(CIV) and NPI(BiO).

#### 4.2.3. Curvature Approximation

The curvature approximation is very different from the HST or NPI schemes in that it does not require computing overlap integrals; all that is needed is the second-order time derivative of adiabatic potential energies. The curvature approximation stems from the Baek-An coupling approximation<sup>6</sup> that was originally derived for 1-dimensional systems by considering the relationship between the Lorentzian dependence of NACs along a

diabatization coordinate and the linear vibronic coupling scheme and conjecturing that the approximation so derived could be useful not only near a diabatic crossing seams but also nearby. By recognizing that a trajectory is 1-dimensional propagation along a time coordinate, one can approximate the TDC in terms of the curvature of the potential energy surfaces along the time coordinate<sup>7,8</sup> (that is why we call it the curvature approximation):

$$\Xi_{IJ}^{\kappa}(t) = \begin{cases} \frac{1}{2} \left[ \frac{d^2 \Delta V_{IJ}(t)}{dt^2} \frac{1}{\Delta V_{IJ}(t)} \right]^{1/2} & \text{for radicand positive} \\ 0 & \text{for radicand negative} \end{cases} \quad (18)$$

$$\sigma_{IJ}^{\kappa}(t) = \Xi_{IJ}^{\kappa}(t) \text{ for } J > I \quad (19)$$

$$\sigma_{IJ}^{\kappa}(t) = -\Xi_{IJ}^{\kappa}(t) \text{ for } J < I \quad (20)$$

where

$$\Delta V_{IJ}(t) = V_I(t) - V_J(t) \quad (21)$$

The curvature approximation to the TDC is called  $\kappa$ TDC.

We can consider two formulas for computing the second-order time derivative of  $\Delta V_{IJ}(t)$ : the *energy formula*,<sup>7,8</sup> which can start at the third step with

$$\frac{d^2 \Delta V_{IJ}(t)}{dt^2} \approx \frac{1}{\Delta t^2} [\Delta V_{IJ}(t) - 2\Delta V_{IJ}(t^-) + \Delta V_{IJ}(t - 2\Delta t)] \quad (22)$$

and at the fourth step switch to

$$\frac{d^2 \Delta V_{IJ}(t)}{dt^2} \approx \frac{1}{\Delta t^2} [2\Delta V_{IJ}(t) - 5\Delta V_{IJ}(t^-) + 4\Delta V_{IJ}(t - 2\Delta t) - \Delta V_{IJ}(t - 3\Delta t)] \quad (23)$$

and the *gradient formula*,<sup>7</sup>

$$\frac{d^2 \Delta V_{IJ}(t)}{dt^2} \approx \frac{\Delta \dot{V}_{IJ}(t) - \Delta \dot{V}_{IJ}(t^-)}{\Delta t} \quad (24)$$

The gradient formula follows from

$$\Delta \dot{V}_{IJ}(t) = \frac{\partial \Delta V_{IJ}(t)}{\partial \mathbf{R}} \cdot \dot{\mathbf{R}} \quad (25)$$

Note that for a small enough step size, these two formulas should give the same result. The gradient formula is more stable numerically than the energy formula because lower-order finite differences are always more stable. However, when one uses the TSH method without spin-orbit coupling with the energy formula, one needs gradients only for the active surface, but the gradient formula requires gradients for all electronic states, which can add to the computational cost. For methods that uses self-consistent potentials,<sup>34,56,57,58,59,60,61,62</sup> or for calculations that include spin-orbit coupling,<sup>50,51,63,64</sup> the gradient formula should be preferred.

We denote the energy  $\kappa$ TDC formula as  $\kappa$ TDC/E and its result as  $\sigma_{IJ}^{\kappa/E}(t)$ ; we denote the gradient  $\kappa$ TDC formula as  $\kappa$ TDC/G and its result as  $\sigma_{IJ}^{\kappa/G}(t)$ .

#### 4.2.4. Local Diabatization scheme

Instead of directly approximating the TDC, the LD scheme performs an adiabatic to diabatic transformation;<sup>24</sup> because such diabaticity is only valid within a time step, the states are locally but not globally diabatic. The locally diabatic states are defined by

$$\mathbf{H}^{\text{LD}}(t^+) = \mathbf{S}(t, t^+) \mathbf{H}(t^+) \mathbf{S}(t, t^+)^{\dagger} \quad (26)$$

One assumes that the electronic coefficients are the same in the adiabatic and diabatic bases at time  $t$ ; then the propagation from time  $t$  to  $t^+$  is carried out diabatically,

$$\dot{\mathbf{c}} = - \left( \frac{i}{\hbar} \mathbf{H}^{\text{elec}} \right) \mathbf{c} \quad (27)$$

As in the HST and NPI schemes, one can use approximated overlap integrals in performing the locally diabatic transformation shown in eq (26).

#### 4.2.5. Summary of Time-Derivative couplings

We have introduced the following schemes to compute or approximate the TDC: analytic scheme, HST scheme, NPI scheme,  $\kappa$ TDC/E formula, and  $\kappa$ TDC/G formula. Furthermore, one can think of the LD scheme as an effective computation of the TDC by constructing a locally diabatic basis. For the schemes using overlap integrals, one may use either exact or approximated overlap integrals, where the HST(CIV) scheme and HST(BiO) scheme are prominent examples of the latter. If one uses exact overlap integrals and a small enough step size, the overlap methods and LD method should yield results identical to the analytic method because the overlap method is an analytically correct way to calculate the needed component of the NAC, but curvature-driven methods differ from the analytic method even for a converged step size because the curvature-driven method involves an approximation to the NAC.

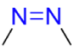
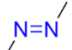
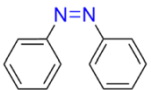
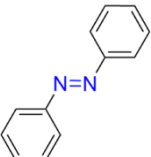
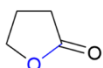
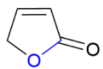
In the above notation, the NAC-based algorithm uses the analytic scheme; the overlap-based algorithms use HST schemes, NPI schemes, or LD schemes (where we use plural “schemes” because of the possibility of using accurate or variously approximated overlap integrals); and the curvature-driven algorithms use  $\kappa$ TDC/E or  $\kappa$ TDC/G formulas.

## 5. Computational Details

We present two sets of simulations in this work. The first set of simulations is like that of ref. 1 except that we use the bug-fixed SHARC-MN v2.0; note that SHARC 3.0 has the same code for these calculations as SHARC-MN v2.0, and thus the calculations could have been equivalently done with SHARC 3.0. The second set of simulations involves a more detailed study of the accuracy of TDC approximations.

In the first set of simulations, six different systems have been studied, namely, *cis*-azomethane (*cis*-AZM), *trans*-azomethane (*trans*-AZM), *cis*-azobenzene (*cis*-AZB), *trans*-azobenzene (*trans*-AZB), butyrolactone, and furanone. All electronic structure calculations are performed with *OpenMolcas*.<sup>41</sup> State averaged complete active space self-consistent field theory (SA-CASSCF)<sup>65,66</sup> is employed for the electronic structure, and the number of states averaged, the active space, and basis set used for each system is summarized in Table 1. Table 1 also gives the number of trajectories in each ensemble and the simulation time. The initial conditions are sampled from the ground-state Wigner distribution implemented with Newton-X<sup>67,68</sup>.

Table 1. Electronic structure and dynamics details for simulation set 1

system	electronic structure calculation		dynamics simulation		
	number of states averaged and active space size	basis set	number of trajectories	simulation time (fs)	
<i>cis</i> -AZM		SA(2)-CASSCF(6,4)	6-31G(d)	100	145
<i>trans</i> -AZM		SA(2)-CASSCF(6,4)	6-31G(d)	200	350
<i>cis</i> -AZB		SA(4)-CASSCF(14,12)	ANO-RCC-VDZP	100	100
<i>trans</i> -AZB		SA(4)-CASSCF(14,12)	ANO-RCC-VDZP	100	100
butyrolactone		SA(3)-CASSCF(10,8)	ANO-RCC-VDZP	200	100
furanone		SA(3)-CASSCF(12,10)	ANO-RCC-VDZP	100	150

For each system, five schemes for computing the TDC are employed, namely, the analytic scheme, LD scheme, HST(CIV) scheme, HST(Bio) scheme, and  $\kappa$ TDC/E formula. (We present only results with the correct SHARC-MN v2.0 and do not repeat the incorrect results from ref 1 caused by the bug in SHARC-MN v1.2.) We used four different dynamics programs as specified with time steps and number of electronic substeps in Table 2.

Table 2. Dynamics methods details for set 1

TDC Scheme	time step (fs)	# of substeps	software
analytic	0.5	100	SHARC 2.1
LD	0.5	1 <sup>a</sup>	Newton-X
HST(CIV)	0.48	96	<i>OpenMolcas</i>
HST(BiO)	0.48	96	<i>OpenMolcas</i>
$\kappa$ TDC/E	0.5	100	SHARC-MN v2.0

<sup>a</sup>The implementation in Newton-X for the LD scheme does not use a substep propagator. It propagates the coefficient over the full time step. See for example, eq 6 of ref 67.

All calculations employed Tully’s fewest-switches version<sup>5</sup> of trajectory surface hopping with an energy-based decoherence correction (EDC).<sup>69</sup> The constant  $C$  in the EDC formula is set to the standard value of 0.1 hartree.

After a hop, nuclear velocity is rescaled along the velocity vector direction in all calculations, and all frustrated hops are ignored. These choices were adopted for consistency with ref 1, but we remind the reader that our preferred choice for momentum adjustment is using a projected NAC<sup>70</sup> when NACs are available, or a projected effective NAC when they are not, and our preferred choice for the treatment of frustrated hops is the  $\nabla V$  scheme.<sup>71</sup> (Projected NACs, projected velocities, and the  $\nabla V$  scheme are all now available in SHARC MN v2.0<sup>9</sup> and SHARC 3.0.<sup>10</sup>)

The second set of simulations is a detailed investigation of the TDC approximations for *cis*-AZM and *trans*-AZM dynamics. Four TDC schemes are compared, namely the LD scheme, NPI scheme,  $\kappa$ TDC/E formula, and  $\kappa$ TDC/G formula. The electronic structure method, dynamics method, and initial condition selection are identical to set 1. The *Molpro*

---

software package is used for SA-CASSCF calculations.<sup>45</sup> We used a locally modified version of SHARC MN v2.0 that enables us to compute all TDCs by different schemes at the same time.

## 6. Results

### 6.1. Ensemble Averaged Population for All Systems

First, as in ref. 1, we study the accuracy of  $\kappa$ TDC/E formula as compared to the other schemes. Table 3 shows the extent of energy nonconservation in the trajectories, and Figure 1 shows the ensemble-averaged populations as functions of time. Notice that the results of the analytic scheme shown in Figure 1 have very small differences from those reported in ref 1 because in ref 1, the analytic scheme was done by Newton-X, whereas in the current study, it is done by SHARC-MN v2.0. All trajectories that failed to conserve energy within 0.5 eV are discarded in the analysis of set 1.

Table 3 reports the percentage of trajectories that fail to conserve energy within a given threshold for each scheme for all six systems. In TSH calculations, the algorithm employed to propagate the electronic coefficients has no direct effect on energy conservation because the trajectory propagates on a single potential energy surface between hops. However, the algorithm does affect active state switches. Since energy conservation is enforced by construction at a hop, the energy nonconservation may be attributed to the regions between hops. For surface-hopping simulations, energy nonconservation may have therefore have more than one source: finite difference error or roundoff in the algorithm with which the nuclear motion is integrated, numerical inexactness of the energy gradients, and – in direct dynamics with SA-CASSCF – energy nonsmoothness of the SCF convergence. In the general case, nonsmoothness of SCF convergence has two possible causes: (i) Sometimes this is due to orbitals that go into or out of the active space. (ii) However, in other situations, some active orbitals and some inactive orbitals may have different mixtures in different steps. In light of these considerations, the relation of energy conservation or nonconservation to the scheme is for evaluating the TDC is complicated, and different algorithms and different molecules may be more or less sensitive to various factors. Upon comparing algorithms, Table 3 shows, nevertheless, that, on average, all methods have similar energy conservation when applied with the same time step, although HST(CIV) does show the worst conservation. Upon

---

comparing molecules, though, there is one exception to the good energy conservation, namely *trans*-AZB; Table 3 shows a larger number of trajectories with poor energy conservation for all schemes for this molecule.

Inspection of the trajectories indicate that error in energy conservation is mostly caused by sudden jumps in potential energy surfaces; however, although in general active orbitals can mix from one time step to the next (within the active space), no rotation of orbitals in and out the active space was observed in the present work, demonstrating a rather stable active space. This indicates that type-ii nonconservation is involved. An example is illustrated in Figure S1 in the SI, which shows a prototypical trajectory that conserves energy better than 0.2 eV, but nevertheless shows this kind of problem. The top panel of Figure S1 is the TDC evaluated by the  $\kappa$ TDC/E formula, and the bottom panel is the potential energy surface as a function of time. The sudden jumps are highlighted with circles in the bottom panel; apparently, these sudden jumps cause artificial local spikes of TDCs. This example shows how one must be careful to distinguish errors caused by the dynamic algorithms, from errors caused by the underlying direct electronic structure calculations, or from the coupling between the two. Indeed, with direct dynamics methods, small or large instabilities in the electronic structure calculations can have consequences on the dynamics results, and different dynamics algorithms have different behaviors with respect to details of electronic structure calculation.

Table 3. Percentages of trajectories that do not conserve energy within a given threshold amount

Threshold	analytic	LD	HST(Bio)	HST(CIV)	$\kappa$ TDC/E
<i>cis</i> -azomethane					
0.5 eV	2	2	3	2	2
0.2 eV	2	2	3	2	3
<i>trans</i> -azomethane					
0.5 eV	2	1	0	0	0
0.2 eV	2	1	0	0	0
<i>cis</i> -azobenzene					
0.5 eV	0	1	3	5	2
0.2 eV	24	19	23	22	21
<i>trans</i> -azobenzene					
0.5 eV	1	7	4	18	12
0.2 eV	34	42	37	63	48
butyrolactone					
0.5 eV	2	1	1	8	1
0.2 eV	11	12	10	23	20
furanone					
0.5 eV	2	1	4	4	3
0.2 eV	6	2	7	8	13
Average					
0.2 eV	13	13	13	20	18
Average omitting <i>trans</i> -AZB					
0.2 eV	9	7	9	11	11



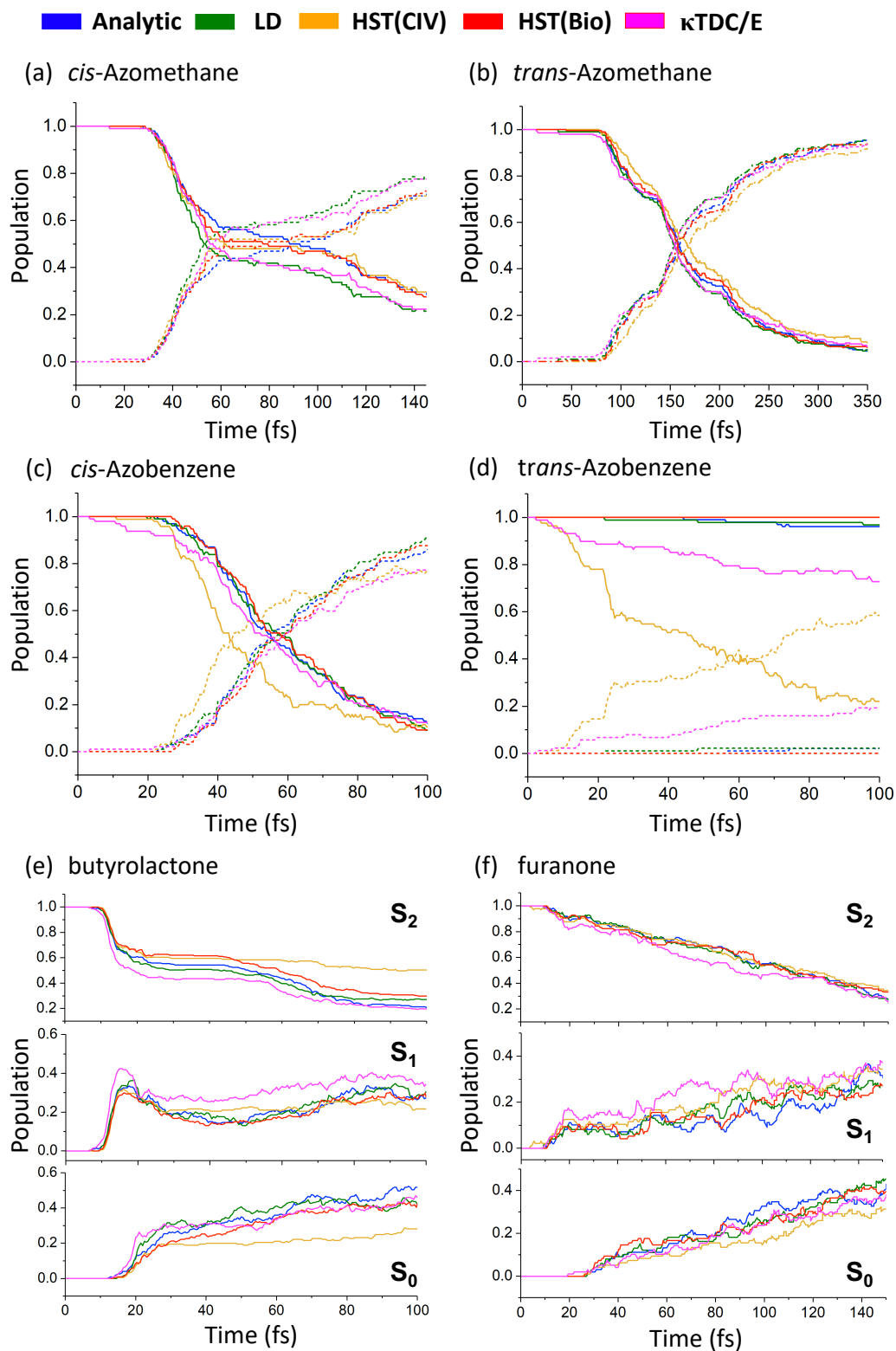


Figure 1. Ensemble-averaged population as a function of time for (a) *cis*-azomethane, (b) *trans*-azomethane, (c) *cis*-azobenzene, (d) *trans*-azobenzene, (e) butyrolactone, (f) furanone. For panels a, b, c, d, the ground-state population is shown as dotted curve. For panels e and f, we show the populations for  $S_0$ ,  $S_1$ , and  $S_2$  in separate subpanels.

Figure 1 shows that  $\kappa$ TDC/E gives accurate time-dependent populations for most systems, with the only exception being *trans*-AZB. The differences are not due to poor energy conservation because trajectories with poor energy conservation are removed from the analysis. Furthermore, the smaller sudden jumps that may still be present are there in all schemes. It seems that the different schemes do not have all the same sensitivity to details of the electronic structure calculations.

We do not discuss the chemical aspects of the photochemical behaviors for the six systems because that is already given in ref 1.

## 6.2 Comparisons of TDCs from Various Schemes

Next, we discuss the dynamics calculation of set 2, which are used to compare TDCs computed by different schemes. All trajectories that failed to conserve energy within 0.2 eV are discarded in the analysis of set 2. We compare TDCs computed by the analytic scheme, the NPI scheme, the  $\kappa$ TDC/E formula, and the  $\kappa$ TDC/G formula. The ensemble averaged population as a function of time for *cis*- and *trans*-AZM is shown in Figure S2 in the SI; the results are very similar to those in panels a and b of Figure 1. (The analytic and  $\kappa$ TDC/E results in Figure 1 and Figure S2 are not the same because the results in Figure S2 are from a different dynamic simulation using *Molpro*.)

To assess the accuracy of the TDC computed by various methods, especially by the curvature-driven approximations, we plotted the TDCs evaluated from  $\kappa$ TDC/E,  $\kappa$ TDC/G, and NPI formulas versus analytic TDCs along the trajectory. The TDC shown in the figures has units of  $1/(\text{aut})$ , where aut is the atomic unit of time, which equals 0.02419 fs. Scatter plots for every time step for the whole ensemble are shown in Figure 2. In Figure 2 we do not include those points correspond to  $\kappa$ TDC equals zero because they cannot be shown in a logarithm plot. To assess the corresponding analytic TDCs of such points, histograms of points with  $\kappa$ TDC/G or  $\kappa$ TDC/E equal to zero are shown in Figure S3 in SI. Clearly these points correspond to small analytic TDC values.

The color of each point in Figure 2 corresponds to the energy gap according to the color bar shown on the right of each panel. We see that the  $\kappa$ TDC/E and  $\kappa$ TDC/G formulas tend to overestimate the TDCs compared with analytic TDC for points where the TDC is small, i.e.,

less than  $10^{-3}$ . However, we expect that the rate of internal conversion is typically dominated by regions where the coupling is large, and inaccuracies in regions where the coupling is weak are expected to have only a small effect on the overall accuracy in most cases.

Therefore, the points that are especially important for photochemical dynamics are those for which the TDC is relatively large. Those are the points toward the upper right of the plots. As expected, they tend to be blue, indicating that they correspond to places where the energy gap is small. For large TDCs and small gaps we see a good correlation of the curvature-driven TDC and the analytic TDC.

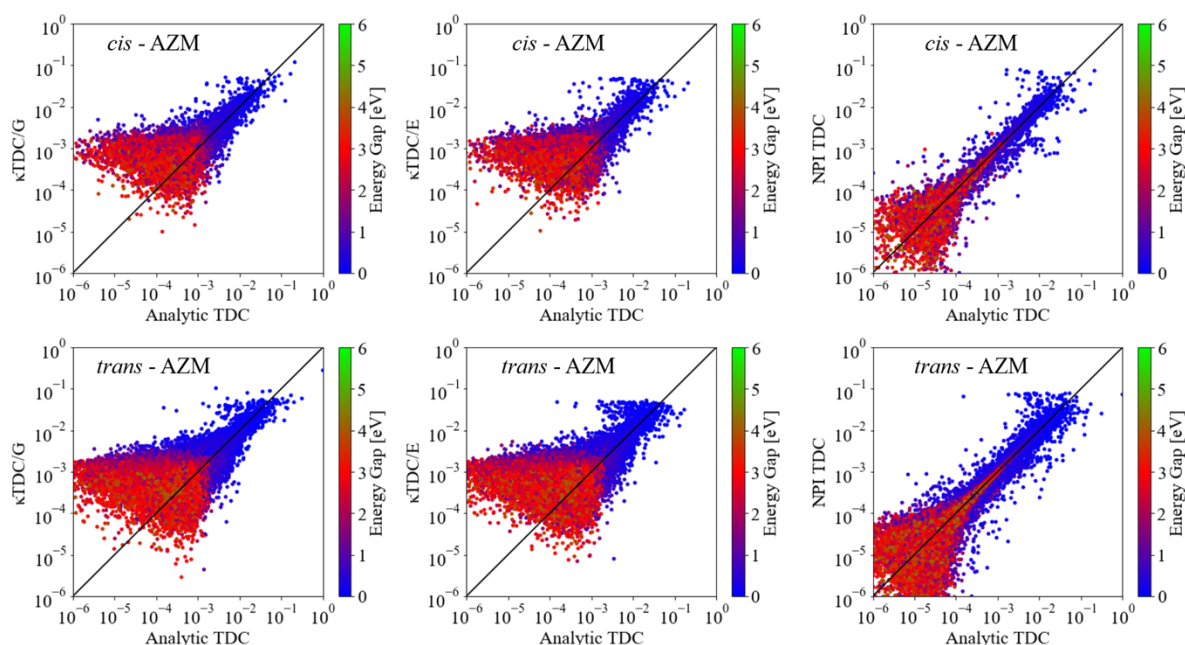


Figure 2. The scatter plot of TDCs evaluated from  $\kappa$ TDC/E (right),  $\kappa$ TDC/G (mid), NPI (right) formulas compared with the analytic TDC for both *cis*- and *trans*-AZM molecule.

Next we compare the curvature-driven algorithms with overlap-based algorithms. Specifically, we investigated the time at which a hop happens for *cis*- and *trans*-AZM trajectories that use  $\kappa$ TDC/E and  $\kappa$ TDC/G approaches as compared to those that use the LD scheme. This is shown in Figure 3. (Although other discussion involves comparing to analytic TDCs, the comparison for when a hop occurs is carried out using LD trajectories because LD trajectories should have no trivial crossing problem. A figure similar to Figure 3 but that compares the hopping time for *cis*- and *trans*-AZM trajectories that use  $\kappa$ TDC/E,  $\kappa$ TDC/G

approaches, and NPI schemes with analytic scheme is shown in Figure S4 in the SI.) The orange and blue points in Figure 3 are for *cis*- and *trans*-AZM respectively. The times are comparable because we used a fixed time step and the same random number seeds for the different methods. Figure 3 shows reasonably good correspondence between the methods.

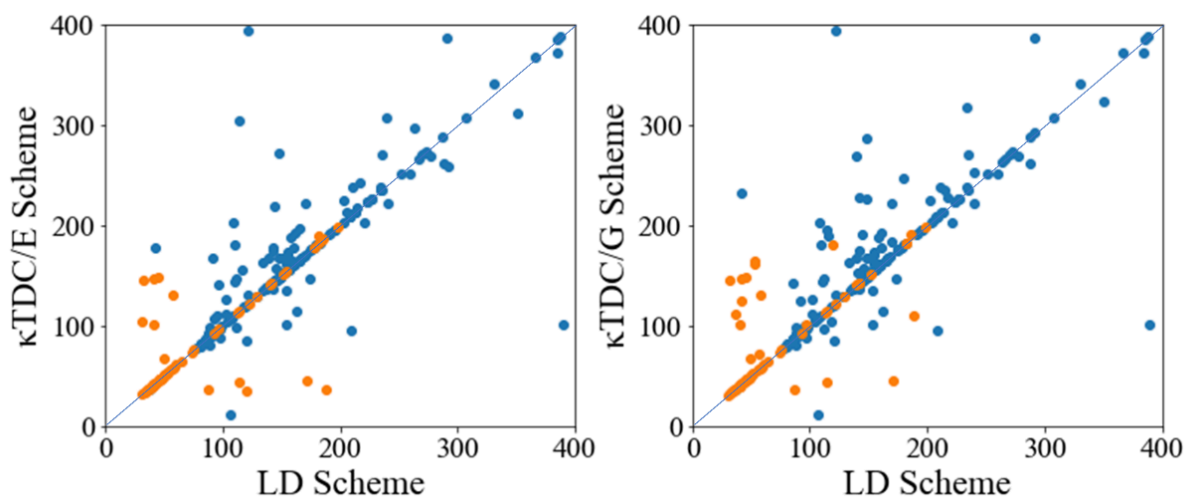


Figure 3. The time (in fs) at which a hop occurs for trajectories that use  $\kappa$ TDC/E (on the left) and  $\kappa$ TDC/G (on the right) formulas as compared to the time at which a hop occurs with the LD scheme. Orange and blue points are for *cis*- and *trans*-AZM respectively.

Figure 4 compares the TDCs evaluated with  $\kappa$ TDC/E and  $\kappa$ TDC/G formulas to the analytic TDCs for the geometries where hops happen in *cis*- and *trans*-AZM trajectories. This figure shows that both  $\kappa$ TDC/E and  $\kappa$ TDC/G approaches are reasonably accurate, but  $\kappa$ TDC/G is generally closer than  $\kappa$ TDC/E to the analytic TDC. The curvature-driven scheme appears to be more accurate when the coupling is large than when it is small. The main limitation of the trajectories in Figure 4 is probably the semiclassical nature of the dynamics algorithms and the propagation on a non-self-consistent potential in surface hopping calculations, not the quantitative values of the coupling constants. The main conclusion to be drawn from Figure 4 is that the curvature-driven approximation works well for most trajectories.

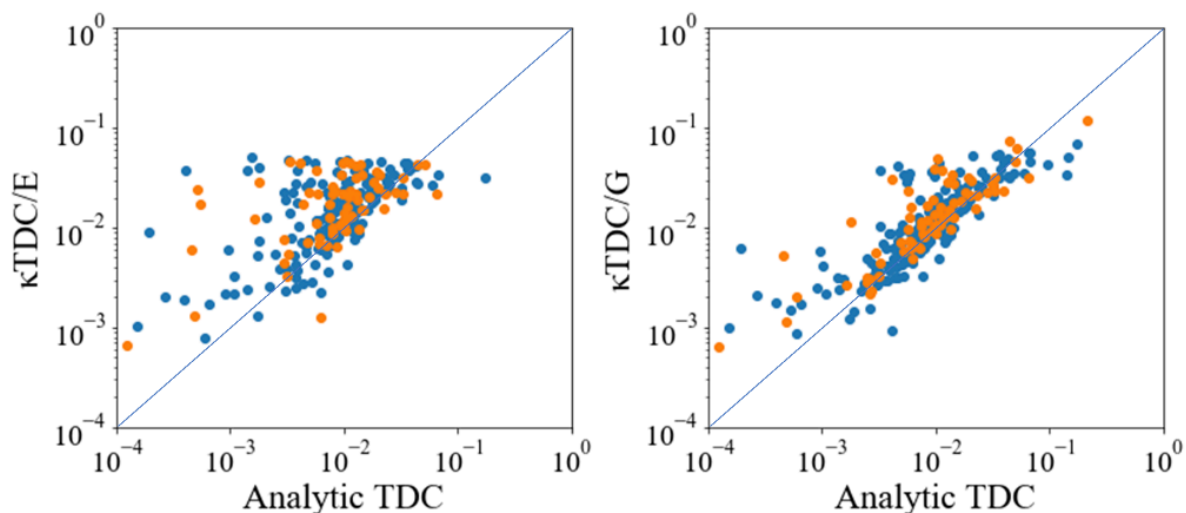


Figure 4. Scatter plot of TDCs evaluated with  $\kappa\text{TDC}/E$  (left) and  $\kappa\text{TDC}/G$  (right) approaches as compared to analytic TDC at the geometries where hop occur. Orange and blue are points for *cis*- and *trans*-AZM trajectories respectively.

Figure 5 shows the TDC and potential energy as functions of time for a randomly selected *cis*-AZM trajectory. A similar plot for *trans*-AZM is shown in Figure S5 in the SI. We see especially good agreement in the important region where the TDC is large. We thus draw the same conclusions as from Figure 4.

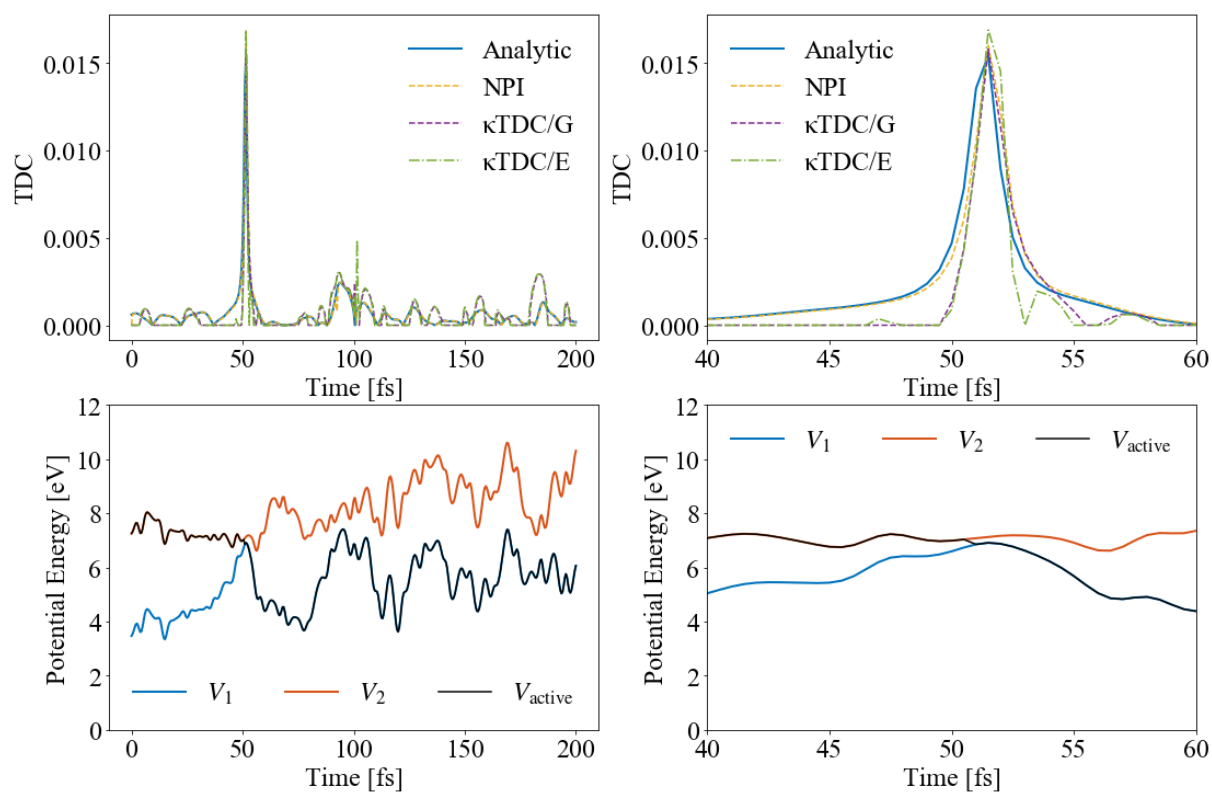


Figure 5. A randomly selected trajectory for *cis*-AZM. The upper left panel shows the TDC evaluated by the analytic scheme, the NPI scheme, and the  $\kappa$ TDC/E and  $\kappa$ TDC/G formulas as functions of time. The upper right panel is a zoom on the region between 40 and 60 fs. The bottom left panel shows the potential energy as a function of time for both ground and excited state as well as the potential energy  $V_{\text{active}}$  of the active state; the bottom right panel zooms this for 40–60 fs.

## 7. Concluding Remarks

We showed that the previous large differences in ensemble populations as functions of time predicted by trajectory surface hopping calculations using the curvature-driven algorithm and by trajectory surface hopping calculations using the NAC-based or overlap-based algorithms is removed when a bug is fixed in SHARC-MN. This work shows that the correct application of the curvature-driven methods leads to good agreement of curvature-driven algorithms with analytic evaluation of the time derivative coupling from NACs, and this good performance is consistent with good performance we have obtained<sup>7,47,49,72</sup> on other problems. We also showed that accurate results can be obtained with both the energy and gradient formulas (denoted as  $\kappa$ TDC/E and  $\kappa$ TDC/G respectively) for the curvature-driven approximations to the time-derivative coupling.

We have demonstrated the accuracy of curvature-driven approximation and the overlap-based approximations not only for ensemble-averaged populations as functions of time but also by examining the times at which hops occur and the magnitudes of TDC along the trajectory. In the regions where the coupling is large, there is good agreement of the couplings obtained analytically from NACs, those obtained from overlap integrals, and those obtained by the curvature-driven formulas.

The curvature-driven approximation to the TDC is available for  $\kappa$ TSH calculations in SHARC-MN v2.0,<sup>9</sup> SHARC 3.0,<sup>10</sup> ANT<sup>73</sup> and Newton-X<sup>67,68</sup> (in Newton-X, the curvature-driven approximation for the TDC is called Baek-An coupling). The curvature-driven approximation to the TDC along with a curvature-driven approximation to an effective NAC<sup>7</sup> is available for  $\kappa$ CSDM calculations (which require all components of the NAC or an effective NAC) is available in SHARC-MN v2.0, SHARC 3.0, and ANT. Use of the curvature-driven approximation eliminates the cost, limited availability, and inconvenience of

using analytic NACs. In addition to expense and inconvenience, even when NACs are available, they present problems due to phases, origin dependence, improper treatment of electronic translation, spurious long-range couplings, and artificial nuclear translational and rotational components, all of which are avoided when using the curvature-driven approximation.

### **Acknowledgments**

This work was performed using HPC resources from GENCI-IDRIS (Grant 2022-101353), CCIPL/Glicid (Le centre de calcul intensif des Pays de la Loire), and Minnesota Supercomputing Institute. I.C.D.M. acknowledges thesis funding from Nantes Université. This work was also supported in part by the U.S. Department of Energy, Office of Science, Office of Basic Energy Sciences under award DE-SC0015997.

## References

- <sup>1</sup> Merritt, I. C. D.; Jacquemin, D.; Vacher, M. Nonadiabatic Coupling in Trajectory Surface Hopping: How Approximations Impact Excited-State Reaction Dynamics. *J. Chem. Theory Comput.* **2023**, *19*, 1827-1842.
- <sup>2</sup> Tully, J. C.; Preston, R. K.; Trajectory Surface Hopping Approach to Nonadiabatic Molecular Collisions: The Reaction of H<sup>+</sup> with D<sub>2</sub>. *J. Chem. Phys.* **1971**, *55*, 562-572.
- <sup>3</sup> Truhlar, D. G.; Duff, J. W.; Blais, N. C.; Tully, J. C.; Garrett, B. C. The Quenching of Na(3<sup>2</sup>P) by H<sub>2</sub>: Interactions and Dynamics. *J. Chem. Phys.* **1982**, *77*, 674-776.
- <sup>4</sup> Blais, N. C.; Truhlar, D. G. Trajectory-Surface-Hopping Study of Na(3p <sup>2</sup>P) + H<sub>2</sub> → Na(3s <sup>2</sup>P) + H<sub>2</sub> (v', j', θ). *J. Chem. Phys.* **1983**, *79*, 1334-1342.
- <sup>5</sup> Tully, J. C. Molecular Dynamics with Electronic Transitions. *J. Chem. Phys.* **1990**, *93*, 1061-1071.
- <sup>6</sup> Baeck, K. K.; An, H. Practical Approximation of the Non-Adiabatic Coupling Terms for Same-Symmetry Interstate Crossings by Using Adiabatic Potential Energies Only. *J. Chem. Phys.* **2017**, *146*, 064107.
- <sup>7</sup> Shu, Y.; Zhang, L.; Chen, X.; Sun, S.; Huang, Y.; Truhlar, D. G. Nonadiabatic dynamics algorithms with only potential energies and gradients: Curvature-driven coherent switching with decay of mixing and curvature-driven trajectory surface hopping. *J. Chem. Theory Comput.* **2022**, *18*, 1320–1328.
- <sup>8</sup> T. do Casal, M.; Toldo, J. M.; Pinheiro, M., Jr; Barbatti, M. Fewest Switches Surface Hopping with Baeck-An Couplings. *Open Res. Europe* **2021**, *1*, 49.
- <sup>9</sup> Shu, Y.; Zhang, L.; Truhlar, D. G. SHARC-MN 2.0; University of Minnesota: Minneapolis, 2023; <https://doi.org/10.5281/zenodo.7818893>.
- <sup>10</sup> Mai, S.; Avagliano, D.; Heindl, M.; Marquetand, P.; Menger, M. F. S. J.; Opperl, M.; Plasser, F.; Polonius, S.; Ruckebauer, M.; Shu, Y. Truhlar, D. G.; Zhang, L.; Zobel, P.; González, L. SHARC 3.0. University of Vienna and University of Minnesota, 2023; <https://doi.org/10.5281/zenodo.7828641>
- <sup>11</sup> Jasper, A. W.; Zhu, C.; Nangia, S.; Truhlar, D. G. Introductory Lecture: Nonadiabatic Effects in Chemical Dynamics. *Faraday Discuss.* **2004**, *127*, 1–22.
- <sup>12</sup> Barbatti, M. Nonadiabatic Dynamics with Trajectory Surface Hopping Method. *Wiley Interdiscip. Rev. Comput. Mol. Sci.* **2011**, *1*, 620–633.
- <sup>13</sup> Tully, J. C. Perspective: Nonadiabatic Dynamics Theory. *J. Chem. Phys.* **2012**, *137*, 22A301.
- <sup>14</sup> Crespo-Otero, R.; Barbatti, M. Recent Advances and Perspectives on Nonadiabatic Mixed Quantum-Classical Dynamics. *Chem. Rev.* **2018**, *118*, 7026–7068.
- <sup>15</sup> Mai, S.; Marquetand, P.; González, L. Nonadiabatic dynamics: The SHARC Approach. *Wiley Interdisc. Rev. Comp. Mol. Sci.* **2018**, *8*, e1370.
- <sup>16</sup> Nelson, T. R.; White, A. J.; Bjorgaard, J. A.; Sifain, A. E.; Zhang, Y.; Nebgen, B.; Fernandez-Alberti, S.; Mozyrsky, D.; Roitberg, A. E.; Tretiak, S. (2020). Non-adiabatic Excited-State Molecular Dynamics: Theory and Applications for Modeling Photophysics in Extended Molecular Materials. *Chem. Rev.* **2020**, *120*, 2215-2287.



- 
- <sup>17</sup> Wang, L.; Qiu, J.; Bai, X.; Xu, J. Surface Hopping Methods for Nonadiabatic Dynamics in Extended Systems. *Wiley Interdisc. Rev. Comp. Mol. Sci.* **2020**, *10*, e1435
- <sup>18</sup> Bian, X.; Wu, Y.; Teh, H.-H.; Zhou, Z.; Chen, H.-T.; Subotnik, J. E. Modeling Nonadiabatic Dynamics with Degenerate Electronic States, Intersystem Crossing, and Spin Separation: A Key Goal for Chemical Physics. *J. Chem. Phys.* **2021**, *154*, 110901.
- <sup>19</sup> Jain, A.; Sindhu, A. Pedagogical Overview of the Fewest Switches Surface Hopping Method. *ACS Omega* **2022**, *7*, 45810-45824.
- <sup>20</sup> Xie, B.-B.; Jia, P.-K.; Wang, K.-X.; Chen, W.-K.; Liu, X.-Y.; Cui, G. Generalized Ab Initio Nonadiabatic Dynamics Simulation Methods from Molecular to Extended Systems. *J. Phys. Chem. A* **2022**, *126*, 1789-1804.
- <sup>21</sup> Shu, Y.; Truhlar, D. G. Decoherence and Its Role in Electronically Nonadiabatic Dynamics. *J. Chem. Theory Comput.* **2023**, *19*, 380-395.
- <sup>22</sup> Chapman, S. The Classical Trajectory–Surface-Hopping Approach to Charge-Transfer Processes. *Adv. Chem. Phys.* **1992**, *82*, 423-483.
- <sup>23</sup> Hammes-Schiffer, S.; Tully, J. C. Proton Transfer in Solution: Molecular Dynamics with Quantum Transitions. *J. Chem. Phys.* **1994**, *101*, 4657-4667.
- <sup>24</sup> Granucci, G.; Persico, M.; Toniolo, A. Direct Semiclassical Simulation of Photochemical Processes with Semiempirical Wave Functions. *J. Chem. Phys.* **2001**, *114*, 10608–10615.
- <sup>25</sup> Zhu, C.; Nobusada, K.; Nakamura, H. (2001). New Implementation of the Trajectory Surface Hopping Method with Use of the Zhu-Nakamura Theory. *J. Chem. Phys.* **2001**, *115*, 3031-3044.
- <sup>26</sup> Lengsfeld, B. H. III; Saxe, P.; Yarkony, D. R. On the Evaluation of Nonadiabatic Coupling Matrix Elements Using SA-MCSCF/CI Wave Functions and Analytic Gradient Methods. I. *J. Chem. Phys.* **1984**, *81*, 4549-4553.
- <sup>27</sup> Lischka, H.; Dallos, M.; Szalay, P. G.; Yarkony, D. R.; Shepard, R. Analytic Evaluation of Nonadiabatic Coupling Terms at the MR-CI Level. I. Formalism. *J. Chem. Phys.* **2004**, *120*, 7322-7329.
- <sup>28</sup> Jasper, A. W.; Truhlar, D. G. Non-Born-Oppenheimer Molecular Dynamics for Conical Intersections, Avoided Crossings, and Weak Interactions. In *Conical Intersections: Theory, Computation, and Experiment*; Domcke, W., Yarkony, D. R., Köppel, H., Eds.; World Scientific: Singapore, 2011; pp. 375-412.
- <sup>29</sup> Plasser, F.; Ruckebauer, M.; Mai, S.; Oettel, M.; Marquetand, P.; González, L. Efficient and Flexible Computation of Many-Electron Wave Function Overlaps. *J. Chem. Theory Comput.* **2016**, *12*, 1207-1219.
- <sup>30</sup> Bao, J. J.; Zhou, C.; Varga, Z.; Kanchanakungwankul, S.; Gagliardi, L.; Truhlar, D. G. Multi-State Pair Density Functional Theory. *Faraday Discuss.* **2020**, *224*, 348-372.
- <sup>31</sup> Bao, J. J.; Zhou, C.; Truhlar, D. G. Compressed-State Multistate Pair-Density Functional Theory. *J. Chem. Theory Comput.* **2020**, *16*, 7444–7452.
- <sup>32</sup> Montavon, G.; Rupp, M.; Gobre, V.; Vazquez-Mayagoitia, A.; Hansen, K.; Tkatchenko, A.; Müller, K.-R.; von Lilienfeld, O. A. Machine Learning of Molecular Electronic Properties in Chemical Compound Space. *New J. Phys.* **2013**, *15*, 095003.
- <sup>33</sup> Kulik, H. J.; Hammerschmidt, T.; Schmidt, J.; Botti, S.; Marques, M. A. L.; Boley, M.; Scheffler, M.; Todorović, M.; Rinke, P.; Oses, C.; Smolyanyuk A.; Curtarolo, S.;

- Tkatchenko, A.; Bartók, A. P.; Manzhos, S.; Ihara, M.; Carrington T.; Behler, J.; Isayev, O.; Veit, M.; Grisafi, A.; Nigam, J.; Ceriotti, M.; Schütt, K. T.; Westermayr, J.; Gastegger, M.; Maurer, R. J.; Kalita, B.; Burke, K.; Nagai, R.; Akashi, R.; Sugino, O.; Hermann, J.; Noé, F.; Pilati, S.; Draxl, C.; Kuban, M.; Rigamonti, S.; Scheidgen, M.; Esters, M.; Hicks, D.; Toher, C.; Balachandran, P. V.; Tamblyn, I.; Whiyelam, S.; Bellinger, C.; Ghiringhelli, L. M. Roadmap on Machine Learning in Electronic Structure. *Electron. Struct.* **2022**, *4*, 023004.
- <sup>34</sup> Zhu, C.; Nangia, S.; Jasper, A. W.; Truhlar, D. G. Coherent Switching with Decay of Mixing: An Improved Treatment of Electronic Coherence for Non-Born-Oppenheimer Trajectories. *J. Chem. Phys.* **2004**, *121*, 7658-7670.
- <sup>35</sup> Fernandez-Alberti, S.; Roitberg, A. E.; Nelson, T.; Tretiak, S. Identification of Unavoided Crossings in Nonadiabatic Photoexcited Dynamics Involving Multiple Electronic States in Polyatomic Conjugated Molecules. *J. Chem. Phys.* **2012**, *137*, 014512.
- <sup>36</sup> Nelson, T.; Fernandez-Alberti, S.; Roitberg, A. E.; Tretiak, S. Artifacts Due to Trivial Unavoided Crossings in the Modeling of Photoinduced Energy Transfer Dynamics in Extended Conjugated Molecules. *Chem. Phys. Lett.* **2013**, *590*, 208–213.
- <sup>37</sup> Wang, L. J.; Prezhdo, O. V. A Simple Solution to the Trivial Crossing Problem in Surface Hopping. *J. Phys. Chem. Lett.* **2014**, *5*, 713–719.
- <sup>38</sup> Meek, G. A.; Levine, B. G. Accurate and Efficient Evaluation of Transition Probabilities at Unavoided Crossings in Ab Initio Multiple Spawning. *Chem. Phys.* **2015**, *16*, 117-124.
- <sup>39</sup> Martínez, T. J. Ab Initio Molecular Dynamics around a Conical Intersection: Li(2p) + H<sub>2</sub>. *Chem. Phys. Lett.* **1997**, *272*, 139-147.
- <sup>40</sup> Malmqvist, P.-Å.; Roos, B. O. The CASSCF State Interaction Method. *Chem. Phys. Lett.* **1989**, *155*, 189–194.
- <sup>41</sup> Li Manni, G.; Galván, I. F.; Alavi, A.; Aleotti, F.; Aquilante, F.; Autschbach, J.; Avagliano, D.; Baiardi, A.; Bao, J. J.; Battaglia, S.; Birnoschi, L.; Blanco-González, A.; Bokarev, S. I.; Broer, R.; Cacciari, R.; Calio, P. B.; Carlson, R. K.; Couto, R. C.; Cerdán, L.; Chibotaru, L.F.; Chilton, N. F.; Church, J. R.; Conti, I.; Coriani, S.; Cuéllar-Zuquin, J.; Daoud, R. E.; Dattani, N.; Decleva, P.; de Graaf, C.; Delcey, M. G.; De Vico, L.; Dobrautz, W.; Dong, S. S.; Feng, R.; Ferré, N.; Filatov M.; Gagliardi, L.; Garavelli, M.; González, L.; Guan, Y.; Guo, M.; Hennefarth, M. R.; Hermes, M. R.; Hoyer, C. E.; Huix-Rotllant, M.; Jaiswal, V. K.; Kaiser, A.; Kaliakin, D. S. Khamesian M.; King, D. S.; Kochetov, V.; Krosnicki, M.; Kumar, A. A.; Larsson, E. D.; Lehtola, S.; Lepetit, M.-B.; Lischka, H.; Ríos, L. P.; Lundberg, M.; Ma, D.; Mai, S.; Marquetand, P.; Merritt, I. C. D.; Montorsi, F.; Mörchen, M.; Nenov, A.; Nguyen, V. H. A.; Nishimoto, Y.; Oakley, M. S.; Olivucci, M.; Oppel, M.; Padula, D.; Pandharkar, R.; Phung, Q. M.; Plasser, F.; Raggi, G.; Rebolini, E.; Reiher, M.; Rivalta, I.; Roca-Sanjuán, D.; Romig, T.; Safari, A. A.; Sánchez-Mansilla, A.; Sand, A. M.; Schapiro, I.; Scott, T. R.; Segarra-Martí, J.; Segatta, F.; Sergentu, D.-C.; Sharma, P.; Shepard, R.; Shu, Y.; Staab, J. K.; Straatsma, T. P.; Sørensen, L. K.; Tenorio, B. N. C.; Truhlar, D. G.; Ungur, L.; Vacher, M.; Veryazov, V.; Voß, T. A.; Weser, O.; Wu, D.; Yang, X.; Yarkony, D.; Zhou, C.; Zobel, J. P.; Lindh, R. The OpenMolcas Web: A Community-Driven Approach to Advancing Computational Chemistry. *J. Chem. Theory Comput.* **2023**, ASAP.
- <sup>42</sup> Meek, G. A.; Levine, B. G. Evaluation of the Time-Derivative Coupling for Accurate

- 
- Electronic State Transition Probabilities from Numerical Simulations. *J. Phys. Chem. Lett.* **2014**, *5*, 2351-2356.
- <sup>43</sup> Shu, Y.; Zhang, L.; Truhlar, D. G. Time-Derivative Coupling for Self-Consistent Electronically Nonadiabatic Dynamics. *J. Chem. Theory Comput.* **2020**, *16*, 4098-4106.
- <sup>44</sup> Levine, B. G.; Coe, J. D.; Virshup, A.; Martínez, T. J. Implementation of Ab Initio Multiple Spawning in the MolPro Quantum Chemistry Package. *Chem. Phys.* 2008, *347*, 3-16.
- <sup>45</sup> Werner, H.-J.; Knowles, P. J.; Knizia, G.; Manby, F. R.; Schütz, M. Molpro: A General-Purpose Quantum Chemistry Program Package. *WIREs Comput. Mol. Sci.* **2012**, *2*, 242-253.
- <sup>46</sup> Garrett, B. C.; Redmon, M. J.; Truhlar, D. G.; Melius, C. F. *Ab Initio* Treatment of Electronically Inelastic K + H Collisions Using a Direct Integration Method for the Solution of the Coupled-Channel Scattering Equations in Electronically Adiabatic Representations. *J. Chem. Phys.* **1981**, *74*, 412-424.
- <sup>47</sup> Zhang, L.; Shu, Y.; Bhaumik, S.; Chen, X.; Sun, S.; Huang, Y.; Truhlar, D. G. Nonadiabatic Dynamics of 1,3-Cyclohexadiene by Curvature-Driven Coherent Switching with Decay of Mixing. *J. Chem. Theory Comput.* **2022**, *18*, 7073-7081.
- <sup>48</sup> Varga, Z.; Shu, Y.; Ning, J.; Truhlar, D. G. Diabatic Potential Energy Surfaces and Semiclassical Multi-State Dynamics for Fourteen Coupled  $^3A'$  states of O<sub>3</sub>. *Electron. Struct.* **2022**, *4*, 047002.
- <sup>49</sup> Zhao, X.; Shu, Y.; Zhang, L.; Xu, X.; Truhlar, D. G. Direct Nonadiabatic Dynamics of Ammonia with Curvature-Driven Coherent Switching with Decay of Mixing and with Fewest Switches with Time Uncertainty: An Illustration of Population Leaking in Trajectory Surface Hopping Due to Frustrated Hops. *J. Chem. Theory Comput.* **2023**, *19*, 1672-1685.
- <sup>50</sup> Mai, S.; Marquetand, P.; González, L.; A General Method to Describe Intersystem Crossing Dynamics in Trajectory Surface Hopping. *Int. J. Quantum Chem.* **2015**, *115*, 1215-1231.
- <sup>51</sup> Shu, Y.; Zhang, L.; Wu, D.; Chen, X.; Sun, S.; Truhlar, D. G. New Gradient Correction Scheme for Electronically Nonadiabatic Dynamics Involving Multiple Spin States. *J. Chem. Theory Comput.* **2023**, *19*, 2419-2429.
- <sup>52</sup> Shu, Y.; Varga, Z.; Kanchanakungwankul, S.; Zhang, L.; Truhlar, D. G. Diabatic States of Molecules. *J. Phys. Chem. A* **2022**, *126*, 992-1018.
- <sup>53</sup> Fabiano, E.; Keal, T. W.; Thiel, W. Implementation of Surface Hopping Molecular Dynamics Using Semiempirical Methods. *Chem. Phys.* **2008**, *349*, 334-347.
- <sup>54</sup> Pittner, J.; Lischka, H.; Barbatti, M. Optimization of Mixed Quantum-Classical Dynamics: Time-Derivative Coupling Terms and Selected Couplings. *Chem. Phys.* **2009**, *356*, 147-152.
- <sup>55</sup> Plasser, F.; Granucci, G.; Pittner, J.; Barbatti, M.; Persico, M.; Lischka, H. Surface hopping dynamics using a locally diabatic formalism: charge transfer in the ethylene dimer cation and excited state dynamics in the 2-pyridone dimer. *J. Chem. Phys.* **2012**, *137*, 22A514.
- <sup>56</sup> Gerber, R. B.; Buch, V.; Ratner, M. A. Time-Dependent Self-Consistent Field Approximation for Intramolecular Energy Transfer. I. Formulation and Application to Dissociation of van der Waals Molecules. *J. Chem. Phys.* **1982**, *77*, 3022-3030.
- <sup>57</sup> Makri, N.; Miller, W. H. Time-Dependent Self-Consistent Field (TDSCF) Approximation for a Reaction Coordinate Coupled to a Harmonic Bath: Single and Multiple Configuration Treatments. *J. Chem. Phys.* **1987**, *87*, 5781-5787.

- 
- <sup>58</sup> Hack, M. D.; Truhlar, D. G. Nonadiabatic Trajectories at an Exhibition. *J. Phys. Chem. A* **2000**, *104*, 7917–7926.
- <sup>59</sup> Li, X.; Tully, J. C.; Schlegel, H. B.; Frisch, M. J. Ab Initio Ehrenfest Dynamics. *J. Chem. Phys.* **2005**, *123*, 084106.
- <sup>60</sup> Ojanperä, A.; Havu, V.; Lehtovaara, L.; Puska, M. Nonadiabatic Ehrenfest Molecular Dynamics within the Projectro Augmented-Wave Method. *J. Chem. Phys.* **2012**, *136*, 144103.
- <sup>61</sup> Makhov, D. V.; Glover, W. J.; Martínez, T. J.; Shalashilin, D. V. Ab Initio Multiple Cloning Algorithm for Quantum Nonadiabatic Molecular Dynamics. *J. Chem. Phys.* **2014**, *141*, 054110.
- <sup>62</sup> Shu, Y.; Zhang, L.; Mai, S.; Sun, S.; González, L.; Truhlar, D. G. Implementation of Coherent Switching with Decay of Mixing into the SHARC Program. *J. Chem. Theory Comput.* **2020**, *16*, 3464–3475.
- <sup>63</sup> Richter, M.; Marquetand, P.; González-Vázquez, J.; Sola, I.; González, L. SHARC: Ab Initio Molecular Dynamics with Surface Hopping in the Adiabatic Representation Including Arbitrary Couplings. *J. Chem. Theory Comput.* **2011**, *7*, 1253–1258.
- <sup>64</sup> Curchod, B. F. E.; Rauer, C.; Marquetand, P.; González, L.; Martínez, T. J. Communication: GAIMS – Generalized Ab Initio Multiple Spawning for Both Internal Conversion and Intersystem Crossing Processes. *J. Chem. Phys.* **2016**, *144*, 101102.
- <sup>65</sup> Ruedenberg, K.; Cheung, L. M.; Elbert, S. T. MCSCF Optimization Through Combined Use of Natural Orbitals and Briouin-Levy-Berthier Theorem. *Int. J. Quantum Chem.* **1979**, *16*, 1069–1101.
- <sup>66</sup> Werner, H.-J.; Meyer, W. A Quadratically Convergent MCSCF Method for the Simultaneous Optimization of Several States. *J. Chem. Phys.* **1981**, *74*, 5794–5801.
- <sup>67</sup> Barbatti, M.; Ruckebauer, M.; Plasser, F.; Pittner, J.; Granucci, G.; Persico, M.; Lischka, H. Newton-X: A Surface-Hopping Program for Nonadiabatic Molecular Dynamics. *Wiley Interdiscip. Rev.: Comput. Mol. Sci.* **2014**, *4*, 26–33.
- <sup>68</sup> Barbatti, M.; Granucci, G.; Ruckebauer, M.; Plasser, F.; Crespo-Otero, R.; Pittner, J.; Persico, M.; Lischka, H. *NEWTON-X: A package for Newtonian Dynamics Close to the Crossing Seam (v.2.2)*; available via the Internet at [www.newtonx.org](http://www.newtonx.org), 2018.
- <sup>69</sup> Granucci, G.; Persico, M. Critical Appraisal of the Fewest Switches Algorithm for Surface Hopping. *J. Chem. Phys.* **2007**, *126*, 134114.
- <sup>70</sup> Shu, Y.; Zhang, L.; Varga, V.; Parkaer, K. A.; Kanchanakungwankul, S.; Sun, S.; Truhlar, D. G. Conservation of Angular Momentum in Direct Nonadiabatic Dynamics. *J. Phys. Chem. Lett.* **2020**, *11*, 1135–1140.
- <sup>71</sup> Jasper, A. W.; Truhlar, D. G. Improved Treatment of Momentum at Classically Forbidden Electronic Transitions in Trajectory Surface Hopping Calculations. *Chem. Phys. Lett.* **2003**, *369*, 60–67.
- <sup>72</sup> Akher, F. B.; Shu, Y.; Varga, Z.; Truhlar, D. G. Semiclassical Multi-State Dynamics for Six Coupled <sup>5</sup>A' States of O + O<sub>2</sub>. *J. Chem. Theory Comput.* **2023**, online as Article ASAP. doi.org/10.1021/acs.jctc.3c00517
- <sup>73</sup> Y. Shu, L. Zhang, J. Zheng, Z.-H. Li, A. W. Jasper, D. A. Bonhommeau, R. Valero, R. Meana-Pañeda, S. L. Mielke, and D. G. Truhlar, *ANT* 2023, University of Minnesota, Minneapolis, 2023. doi.org/10.5281/zenodo.7807406

ToC graphic:

